



HAL
open science

Uridylation and PABP cooperate to repair mRNA deadenylated ends in Arabidopsis.

Hélène Zuber, Hélène Scheer, Emilie Ferrier, Francois Sement, P Mercier, Benjamin Stupfler, Dominique Gagliardi

► **To cite this version:**

Hélène Zuber, Hélène Scheer, Emilie Ferrier, Francois Sement, P Mercier, et al.. Uridylation and PABP cooperate to repair mRNA deadenylated ends in Arabidopsis.. Cell Reports, 2016, 14 (11), pp.2707-2717. 10.1016/j.celrep.2016.02.060 . hal-02185924

HAL Id: hal-02185924

<https://hal.science/hal-02185924>

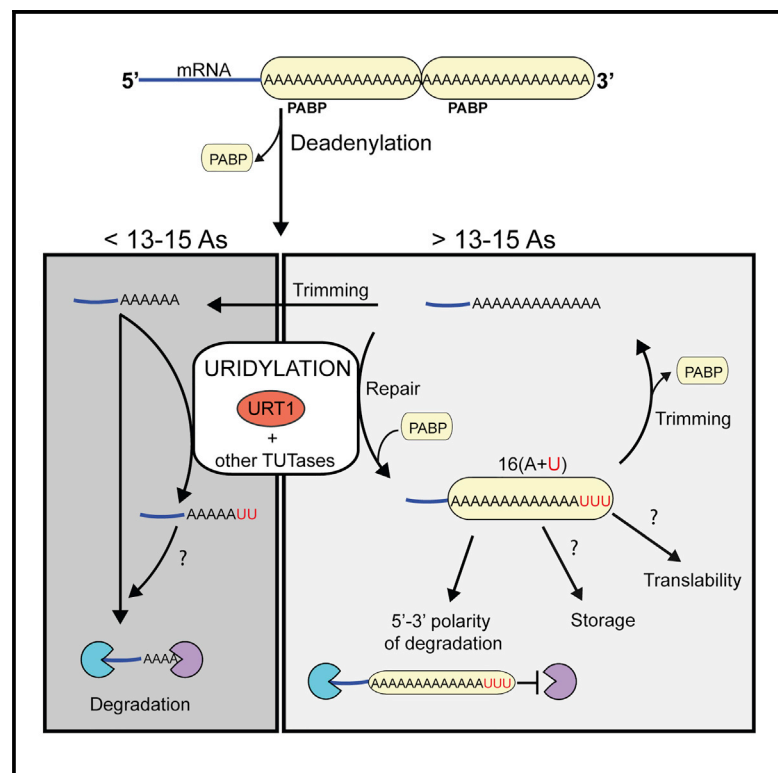
Submitted on 16 Jul 2019

HAL is a multi-disciplinary open access archive for the deposit and dissemination of scientific research documents, whether they are published or not. The documents may come from teaching and research institutions in France or abroad, or from public or private research centers.

L'archive ouverte pluridisciplinaire **HAL**, est destinée au dépôt et à la diffusion de documents scientifiques de niveau recherche, publiés ou non, émanant des établissements d'enseignement et de recherche français ou étrangers, des laboratoires publics ou privés.

Uridylation and PABP Cooperate to Repair mRNA Deadenylated Ends in *Arabidopsis*

Graphical Abstract



Authors

Hélène Zuber, Hélène Scheer, Emilie Ferrier, François Michaël Sement, Pierre Mercier, Benjamin Stupfler, Dominique Gagliardi

Correspondence

dominique.gagliardi@ibmp-cnrs.unistra.fr

In Brief

Zuber et al. report that uridylation can repair deadenylated mRNAs in *Arabidopsis*. Uridylation and poly(A) binding proteins (PABP) cooperate to restore a defined tail length and control the extent of mRNA deadenylation.

Highlights

- TAIL-seq analysis reveals widespread mRNA uridylation in *Arabidopsis*
- Uridylation repairs mRNA deadenylated 3' ends
- PABP binds to uridylated oligo(A) tails and determines the size of U-tail extension
- Uridylation determines the extent of mRNA deadenylation

Accession Numbers

GSE72458



Uridylation and PABP Cooperate to Repair mRNA Deadenylated Ends in *Arabidopsis*

Hélène Zuber,¹ Hélène Scheer,¹ Emilie Ferrier,¹ François Michaël Sement,¹ Pierre Mercier,¹ Benjamin Stupfler,¹ and Dominique Gagliardi^{1,*}

¹Institut de Biologie Moléculaire des Plantes, Centre National de la Recherche Scientifique (CNRS), Université de Strasbourg, 67000 Strasbourg, France

*Correspondence: dominique.gagliardi@ibmp-cnrs.unistra.fr
<http://dx.doi.org/10.1016/j.celrep.2016.02.060>

This is an open access article under the CC BY-NC-ND license (<http://creativecommons.org/licenses/by-nc-nd/4.0/>).

SUMMARY

Uridylation emerges as a key modification promoting mRNA degradation in eukaryotes. In addition, uridylation by URT1 prevents the accumulation of excessively deadenylated mRNAs in *Arabidopsis*. Here, we show that the extent of mRNA deadenylation is controlled by URT1. By using TAIL-seq analysis, we demonstrate the prevalence of mRNA uridylation and the existence, at lower frequencies, of mRNA cytidylation and guanylation in *Arabidopsis*. Both URT1-dependent and URT1-independent types of uridylation co-exist but only URT1-mediated uridylation prevents the accumulation of excessively deadenylated mRNAs. Importantly, uridylation repairs deadenylated extremities to restore the size distribution observed for non-uridylated oligo(A) tails. In vivo and in vitro data indicate that Poly(A) Binding Protein (PABP) binds to uridylated oligo(A) tails and determines the length of U-extensions added by URT1. Taken together, our results uncover a role for uridylation and PABP in repairing mRNA deadenylated ends and reveal that uridylation plays diverse roles in eukaryotic mRNA metabolism.

INTRODUCTION

The control of mRNA stability and translatability is crucial for regulating genome expression. Primary determinants of mRNA stability and translation are the 5' m⁷G cap and the 3' poly(A) tail. These structures are bound by the eukaryotic initiation factor 4E (eIF4E) and poly(A) binding proteins (PABP), respectively. eIF4E contacts eIF4G, which also interacts with PABP, thereby circularizing mRNAs into a stable and translatable entity (Manus et al., 2003). mRNA stability and translation can be modulated by RNA binding proteins and miRNAs. Besides these well-studied transactors, mRNA fate is also regulated by RNA modifications such as the chemical modification of nucleotides and the post-transcriptional untemplated 3' addition of ribonucleotides or tailing (Lee et al., 2014; Norbury, 2013; Munoz-Tello et al., 2015; Viegas et al., 2015). Tailing includes non-canonical

adenylation, which is a widespread modification present in the three domains of life. It triggers the degradation of non-coding RNAs in almost all genetic systems but also the destruction of mRNAs in bacteria, in most Archaea, in chloroplasts and in plant and human mitochondria (Lange et al., 2009; Norbury, 2013). In addition, cytoplasmic adenylation is crucial for activating translation of target mRNAs at several developmental or physiological transitions including oocytes maturation or synapse function (Charlesworth et al., 2013). Besides tailing by adenylation, guanylation and cytidylation of mRNAs have also been recently described in humans, and their respective roles remain to be elucidated (Chang et al., 2014). By contrast, accumulating evidence points toward a role of uridylation in influencing mRNA stability. The uridylation of mRNAs was first demonstrated for human cell-cycle-dependent histone mRNAs, which are not polyadenylated (Mullen and Marzluff, 2008). With reports in *Schizosaccharomyces pombe*, *Aspergillus nidulans*, *Arabidopsis thaliana*, *Trypanosoma brucei*, and humans, it is now evident that uridylation of polyadenylated mRNAs also exists and is a conserved feature of mRNA metabolism in eukaryotes (Chang et al., 2014; Knüsel and Roditi, 2013; Morozov et al., 2010, 2012; Rissland and Norbury, 2009; Sement et al., 2013; Thomas et al., 2015). The TAIL sequencing (TAIL-seq) method, designed to detect transcriptome-wide nucleotide tailing, revealed the pervasiveness of uridylation for human mRNAs (Chang et al., 2014). Human mRNAs are uridylated by both TUT4 and TUT7. Their simultaneous downregulation increases global mRNA half-lives, demonstrating the impact of uridylation in influencing mRNA degradation (Lim et al., 2014). Importantly, uridylation triggers both 5'-3' and 3'-5' mRNA degradation in *S. pombe* and humans (Lim et al., 2014; Malecki et al., 2013; Mullen and Marzluff, 2008; Rissland and Norbury, 2009; Slevin et al., 2014; Su et al., 2013).

Triggering mRNA degradation by uridylation is likely conserved in plants, although this remains to be formally demonstrated. Yet, we recently proposed a role for uridylation in preventing the trimming of oligoadenylated mRNAs in *Arabidopsis* (Sement et al., 2013). We identified UTP:RNA URIDYLYLTRANSFERASE1 (URT1) as the main Terminal Uridyl(yl)Transferase (TUTase) responsible for mRNA uridylation in *Arabidopsis*. *urt1* mutants accumulate mRNAs that are excessively deadenylated, although their decay rate is not affected (Sement et al., 2013). In the present study, we show that URT1

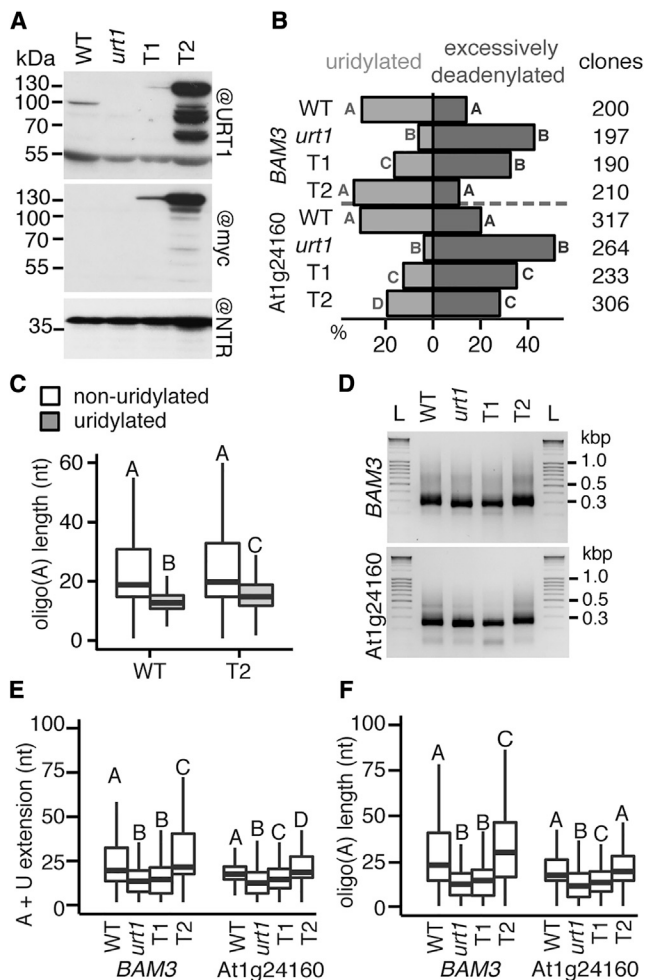


Figure 1. URT1-Mediated Uridylation Modulates the Population of Deadened mRNAs

(A) Transgenic lines T1 and T2 express different levels of myc-URT1. Western blot analysis of WT, *urt1*, T1, and T2 flowers using anti-URT1 and anti-myc antibodies. Antibodies against NADPH-dependent thioredoxin reductase AtNTRB (NTR) were used for controlling loading.

(B) Uridylation and accumulation of excessively deadenylated mRNAs are linked to URT1 expression level. Percentage of uridylated mRNAs (left, in light gray) or excessively deadenylated (from 0 to 10 As) mRNAs (right, in dark gray) determined by 3' RACE-PCR for *BAM3* (At4g20270) and *At1g24160*. The number of analyzed clones for two to three biological replicates (see Supplemental Experimental Procedures) is indicated for each gene and genotype. Significant differences determined by chi-square contingency table tests are indicated by letters.

(C) Deadenylation precedes URT1-mediated uridylation in both WT and T2. Boxplot analysis of poly(A) length distribution for non-uridylated (white) or uridylated (gray) *BAM3* and *At1g24160* mRNAs in WT and T2 lines. The upper and lower edges correspond to the first and third quartiles, respectively. The median is indicated by a horizontal bar and whiskers show data range except for outliers. Significant differences determined by Mann-Whitney tests are indicated by letters.

(D–F) Progressive recovery of tail sizes from *urt1* to T1 and T2. (D) 3' RACE-PCR profiles for *BAM3* and *At1g24160* from flower samples. Negative images of ethidium bromide stained agarose gels. L, DNA ladder. (E and F) Boxplot analysis showing extension sizes for uridylated and non-uridylated sequences (E, poly(A) tail + Us) and for non-uridylated sequences (F, only As) in WT, *urt1*, T1, and T2 lines for *BAM3* and

controls the extent of mRNA deadenylation. By applying TAIL-seq analysis to *Arabidopsis*, we identified two types of uridylation. Only URT1-mediated uridylation prevents the accumulation of excessively deadenylated mRNAs. More importantly, we show that uridylation repairs deadenylated ends to restore a binding site for Poly(A) Binding Protein (PABP). Our results support a model in which uridylation and PABP cooperate to control the extent of mRNA deadenylation in *Arabidopsis*.

RESULTS

URT1-Mediated Uridylation Modulates the Population of Deadened mRNAs

To get further insight into the role of URT1-mediated uridylation, we complemented the *urt1-1* mutant with a myc-tagged version of URT1 and selected two lines with highly dissimilar expression levels of the transgene. Transgenic line T1 expresses myc-URT1 to a lower level than the endogenous URT1 in wild-type (WT), while line T2 overexpresses the transgenic protein (Figure 1A). We then determined the uridylation status of two mRNAs, *BAM3* (At4g20270) and *At1g24160*, previously shown to be targets of URT1 (Sement et al., 2013). The uridylation status of *BAM3* and *At1g24160* in WT, *urt1*, T1, and T2 was determined from 797 and 1,120 clones obtained by using a modified 3' rapid amplification of cDNA ends (RACE)-PCR protocol designed to detect nucleotides added 3' to poly(A) tails (Sement and Gagliardi, 2014). In agreement with previous results, uridylation of both *BAM3* and *At1g24160* is detected in WT and decreases sharply in *urt1* mutant, because URT1 is the main uridylyltransferase responsible for the uridylation of these two mRNAs (Figure 1B). Interestingly, we observed a gradual increase in the level of uridylation from *urt1* to T1 and T2 lines (Figure 1B). In addition, the accumulation of excessively deadenylated mRNAs (defined as mRNAs with an oligo(A) tail from 0 to 10) (Sement et al., 2013) is inversely correlated to the uridylation status in all samples ($r = -0.98$; p value = $1.68E-05$) (Figure 1B). Therefore, varying the expression level of URT1 modulates both the extent of uridylation and the accumulation of excessively deadenylated *BAM3* and *At1g24160* mRNAs. Yet, uridylation in line T2 was not dramatically increased as compared to WT, albeit T2 overexpresses myc-URT1 well above WT endogenous level (Figures 1A and 1B). A possible explanation is that the deadenylation step, which precedes URT1-mediated uridylation (Sement et al., 2013), remains limiting. Confirming this hypothesis, a significant reduction in the poly(A) size for uridylated tails as compared with non-uridylated ones is still observed in T2 (Figure 1C). Therefore, deadenylation appears as a prerequisite for URT1-mediated uridylation.

The accumulation of excessively deadenylated mRNAs in *urt1* as compared to WT can be visualized on agarose gels as a slight shift downward due to the faster migration of shorter 3' RACE-PCR products that correspond to oligoadenylated mRNAs (Figure 1D). A gradual delay in the migration of these 3' RACE-PCR products is observed from *urt1* to lines T1 and T2 (Figure 1D).

At1g24160. Significant differences determined by Mann-Whitney tests are indicated by letters. See also Figure S1.

This increase is solely due to the modification of extension sizes since the position of poly(A) sites are identical in the four genotypes (Figure S1A). Plotting the tail sizes (adenosines and uridines) shows that the 3' extensions of *BAM3* and At1g24160 mRNAs are gradually increased from *urt1* to lines T1 and T2, mirroring myc-URT1 expression levels (Figure 1E). A gradual increase in extension sizes is also observed when considering only non-uridylated poly(A) tails (Figure 1F). This is consistent with the proposed role of URT1 in preventing trimming of oligoadenylated mRNAs. Alternatively, uridylation could also favor the decay of excessively deadenylated mRNAs, thereby shifting upward the population of deadenylated mRNAs. However, the size of uridylated oligo(A) tails is also slightly, but significantly, increased in T2 as compared with WT (Figures 1C and S1B). This observation strongly supports the idea that URT1 overexpression can antagonize the deadenylation step. In conclusion, URT1 expression level influences the sizes of both uridylated and non-uridylated oligo(A) tails. These data do not rule out the possibility that uridylation could trigger the decay of excessively deadenylated mRNAs. However, they also support the idea that URT1-mediated uridylation determines the extent of deadenylation and that an initial deadenylation step cannot be overcome, regardless of URT1 expression level.

Widespread Uridylation of mRNAs in *Arabidopsis*

To obtain a global view of mRNA uridylation in *Arabidopsis*, we generated TAIL-seq libraries from WT plants, *urt1* and *xrn4* single mutants, and *urt1 xrn4* double mutant. The TAIL-seq protocol was recently developed to deep sequence the 3' ends of RNAs (Chang et al., 2014). Briefly, rRNA-depleted RNA samples are ligated to a biotinylated 3' adaptor and fragmented, and the affinity-purified 3' most fragments are ligated to a 5' adaptor prior to cDNA synthesis and library amplification. Paired-end sequencing of TAIL-seq libraries allows the identification of the RNA (read 1) and the analysis of any nucleotides added at its 3' extremity (read 2) (Chang et al., 2014). Because URT1-mediated uridylation occurs on mRNAs with short poly(A) tails (Sement et al., 2013), uridylation of oligoadenylated mRNAs was determined using a base-call analysis protocol, which is suitable for analyzing poly(A) tails up to 30 As (Figure S2) (Chang et al., 2014). As detailed in Supplemental Experimental Procedures, we obtained reads for 2,716, 5,501, 2,571, and 4,077 unique genes in WT, *urt1*, *xrn4*, and *urt1 xrn4* libraries, respectively, though most genes had a low number of reads preventing a reliable gene-to-gene comparison between the four libraries. However, when reads are considered globally, our TAIL-seq data provide an unbiased view of mRNA modification by nucleotide addition in *Arabidopsis*. As detailed below, uridylation emerges as the most common modification. We also observed that about 5% and 2% of the reads of all libraries correspond to guanylated and cytidylated mRNAs, respectively (Figure 2A). A similar observation was recently reported in humans (Chang et al., 2014), indicating that mRNA guanylation and cytidylation is conserved from plants to human.

About one-third of the reads (32%) for mRNAs with poly(A) tails <31 As corresponded to uridylated sequences in WT (Figure 2A). The proportion of uridylated mRNAs drops to 7% in *urt1*, confirming that URT1 is the main terminal uridylyltransfer-

ase modifying mRNAs (Figure 2A). The residual uridylation detected in the *urt1-1*-null mutation indicates that *Arabidopsis* contains at least a second enzyme able to uridylylate mRNAs. In *xrn4*, the ratio of uridylated mRNAs raises to 40%, suggesting that mRNA uridylation is favored when 5'-3' RNA degradation is compromised, as recently reported in humans (Lim et al., 2014). To determine the relative contribution of URT1 in uridylylating mRNAs in *xrn4*, the TAIL-seq analysis was also performed for *urt1 xrn4*. Uridylation drops from 40% in *xrn4* to 13% in *urt1 xrn4* revealing that URT1 is indeed partially responsible for the uridylation observed in *xrn4* and confirming the existence of at least a second TUTase involved in mRNA uridylation (Figure 2A).

Plotting the frequency of uridylation against the poly(A) length unambiguously shows at genomic scale that mRNA uridylation in WT occurs preferentially on oligoadenylated mRNAs (Figure 2B). Indeed, uridylation increases for tail lengths shorter than 20 As and peaks at 11 As, representing about 75% of the reads at this tail length. In *xrn4* as well, uridylation is detected mostly on oligoadenylated mRNAs (Figure 2B). The TAIL-seq data for *xrn4* also reveal that the absence of XRN4 increases the frequency of uridylated mRNAs with short tails. For instance, more than 50% of reads for mRNAs with an oligo(A) tail of six to seven As are uridylated (Figure 2B). In *urt1 xrn4*, the distribution of uridylated oligo(A) tails is also biased toward short tails, as observed in WT and *xrn4* (Figure 2B). The higher proportion of shorter tails that are uridylated in *xrn4* versus WT and in *urt1 xrn4* versus *urt1* can be explained by two alternative, but not mutually exclusive, possibilities: (1) uridylation favors 5'-3' degradation and/or (2) the degradation of deadenylated mRNAs is compromised in the absence of XRN4 and those mRNAs are longer accessible for uridylation. The bias toward shorter tails could also be influenced by an intrinsic preference of the second TUTase for short tails, similar to what is observed for URT1. Interestingly, uridylation drops for oligo(A) tails of 8 nt both in *xrn4* and to a lesser extent in WT (Figure 2B). This drop in uridylation could reveal the binding of a factor that could mask 8-nt A-tails and hinder accessibility by TUTases.

Besides mRNAs, URT1 has recently been identified as uridylylating miRNAs in the absence of the small RNA methyltransferase HEN1 and the uridylyltransferase HESO1 (Tu et al., 2015; Wang et al., 2015). To directly compare the impact of URT1-mediated uridylation on mRNAs and small RNAs, we deep sequenced small RNA libraries for WT and *urt1* duplicate samples at the same developmental stage that was analyzed by TAIL-seq, i.e., 2-week-old seedlings. The overall level of nucleotide tailing of miRNAs was not significantly affected by the lack of URT1 (Figure 2C). No significant changes were observed for ten miRNAs displaying the highest uridylation percentage (>10%) and for eight small interfering RNA (siRNA) loci with at least 40 reads corresponding to uridylated siRNAs (Figures 2D and 2E). Therefore, at the seedling stage investigated here, URT1 is dispensable for bulk small RNA uridylation in a WT context. This observation is in agreement with the recent studies reporting that HESO1 will outcompete URT1 for miRNA tailing (Tu et al., 2015; Wang et al., 2015). Taken together, these data show that URT1 appears dispensable for bulk small RNA uridylation,

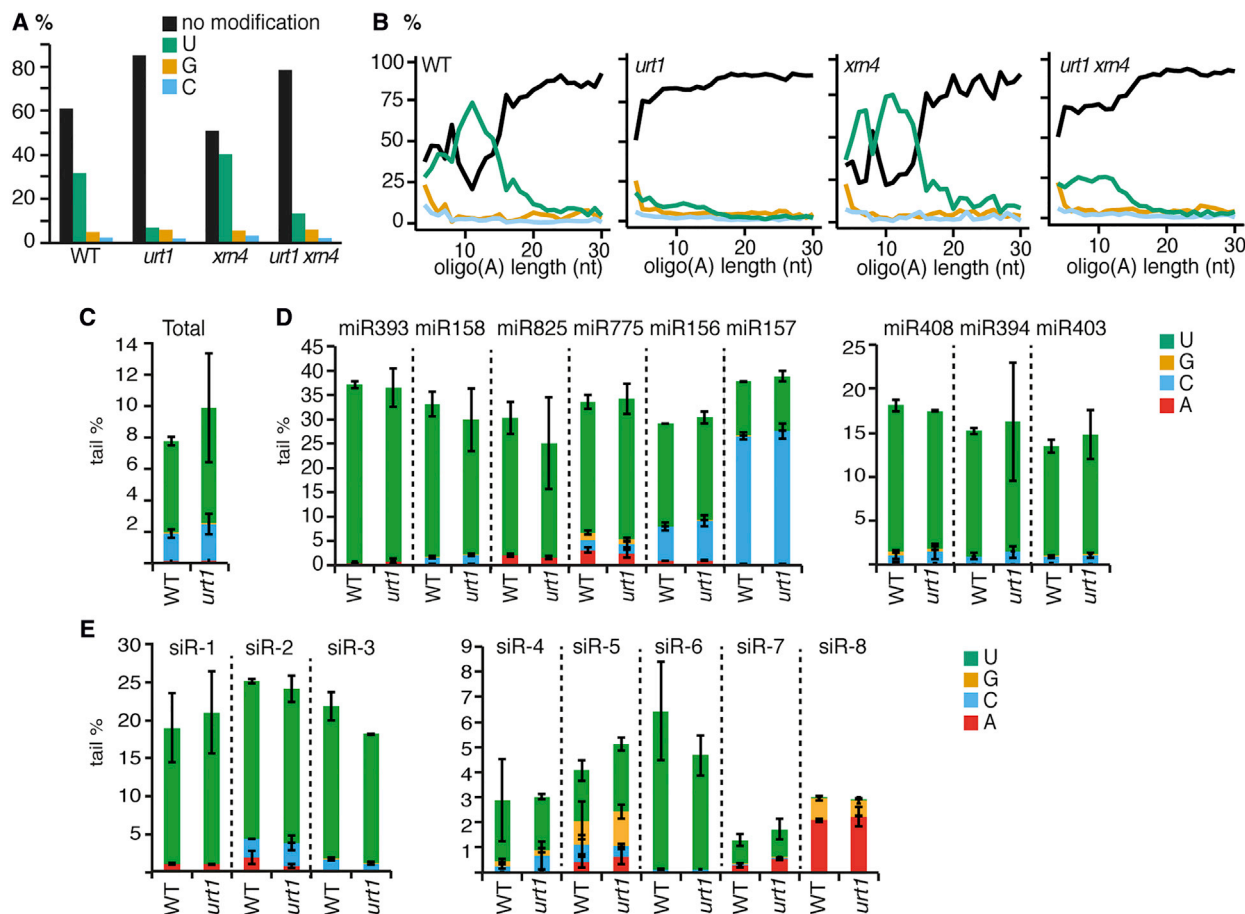


Figure 2. Widespread Uridylation of Oligoadenylated mRNAs in Arabidopsis

(A) Frequency of modifications at mRNA 3' ends for WT, *urt1*, *xrn4*, and *urt1 xrn4* as determined by TAIL-seq analysis.

(B) Frequency of 3' end modifications plotted against poly(A) tail sizes calculated from TAIL-seq analysis. Note that mRNAs with zero to three As are not considered during TAIL-seq data processing (see Supplemental Experimental Procedures).

(C–E) Frequency of the different modifications at the 3' end of miRNAs and siRNAs for WT and *urt1*, two biological replicates each. For all panels, Mann-Whitney tests show no significant differences of tailing between WT and *urt1*. (C) Overall frequency of miRNA tailing. Modification frequencies were calculated as percentage of the total number of reads mapping to miRNAs. (D) Tailing frequency for the ten miRNAs that show the highest uridylation level (>10%). Modification frequencies were calculated for each individual miRNA as percentage of the total number of reads for the corresponding miRNA. (E) Tailing frequency for eight siRNA loci. Modification frequencies were calculated for each individual siRNA loci as percentage of the total number of reads for the corresponding siRNA. See also Figure S2.

whereas it plays a prominent role in mRNA uridylation as shown by TAIL-seq analysis.

Distinct Roles for URT1-Dependent and URT1-Independent Uridylation of mRNAs

The TAIL-seq analysis also revealed the existence of at least a second TUTase involved in mRNA uridylation, besides URT1. This second TUTase(s) cannot fully complement the absence of URT1 because excessively deadenylated mRNAs accumulate in *urt1* single mutants (Sement et al., 2013; Figure 1). This accumulation in *urt1* can be explained either because URT1-mediated and URT1-independent uridylation do not have fully redundant functions or because of a lower global uridylation of mRNAs observed in absence of URT1 (Figure 2A). To distinguish between these possibilities, we took advantage of the increased mRNA uridylation detected in absence of

XRN4, and we looked for individual mRNAs with similar uridylation levels in WT and *urt1 xrn4*. For five model mRNAs investigated by 3' RACE-PCR, uridylation is detected in WT, drops in *urt1*, and increases in *xrn4* and is increased in *urt1 xrn4* as compared to *urt1* (Figure 3A). Yet, uridylation level is not significantly different between WT and *urt1 xrn4* for four out of the five mRNAs (Figure 3A). By contrast, a significant increase in excessively deadenylated mRNAs is observed in *urt1 xrn4* as compared to WT (Figure 3A). In addition, both the migration of shorter 3' RACE-PCR products (Figure 3B) and the analysis of poly(A) sizes (Figure 3C) show that the five mRNAs have shorter oligo(A) tails in *urt1 xrn4* as compared to WT. However, for both migration of PCR products and size of oligo(A) tails, we observed no significant differences between *urt1* and *urt1 xrn4*. These results indicate that URT1-mediated and URT1-independent types of uridylation play distinct roles, with only

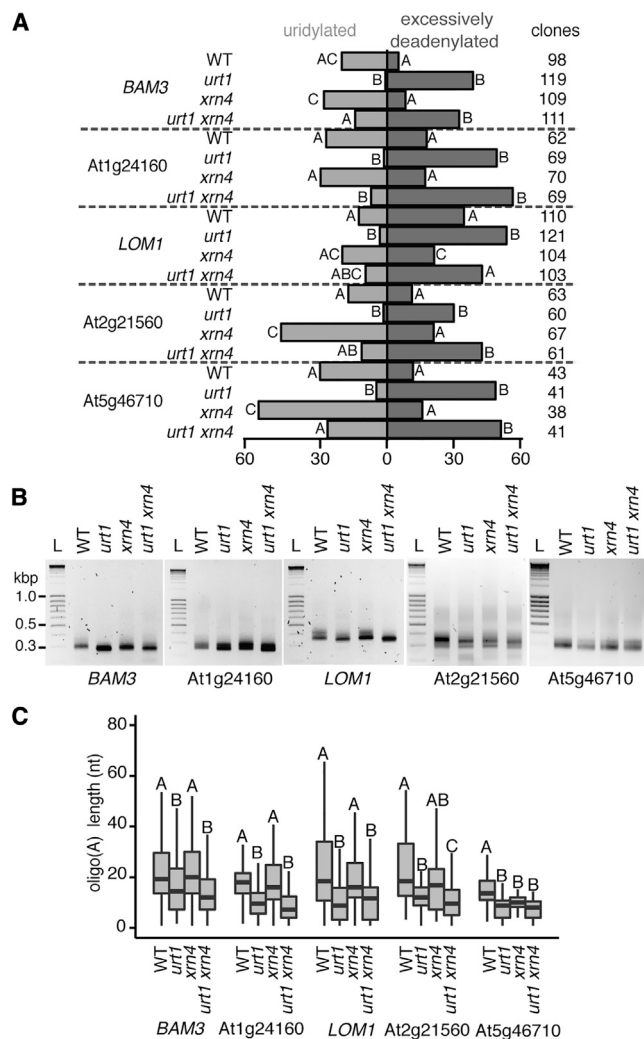


Figure 3. Distinct Roles for URT1-Dependent and URT1-Independent Uridylation of mRNAs

3' RACE-PCR experiments were performed using leaf RNA from two biological replicates from WT, *urt1*, *xrn4*, and *urt1 xrn4* plants. Five model genes were analyzed: *BAM3*, *At1g24160*, *LOM1*, *At2g21560*, and *At5g46710*.

(A) Only URT1-mediated uridylation prevents accumulation of excessively deadenylated mRNAs. Percentage of uridylated mRNAs (light gray) or excessively deadenylated (from 0 to 10 As) mRNAs (dark gray) determined by 3' RACE PCR. The number of analyzed clones is indicated for each gene and genotype. Significant differences determined by chi-square contingency table tests are indicated by letters.

(B) 3' RACE-PCR profiles. Negative images of ethidium bromide stained agarose gels. L, DNA ladder.

(C) Boxplot analysis showing poly(A) sizes for non-uridylated sequences. Significant differences determined by Mann-Whitney tests are indicated by letters.

URT1-mediated uridylation preventing the accumulation of excessively deadenylated mRNAs.

Uridylation Repairs Deadenylated mRNAs

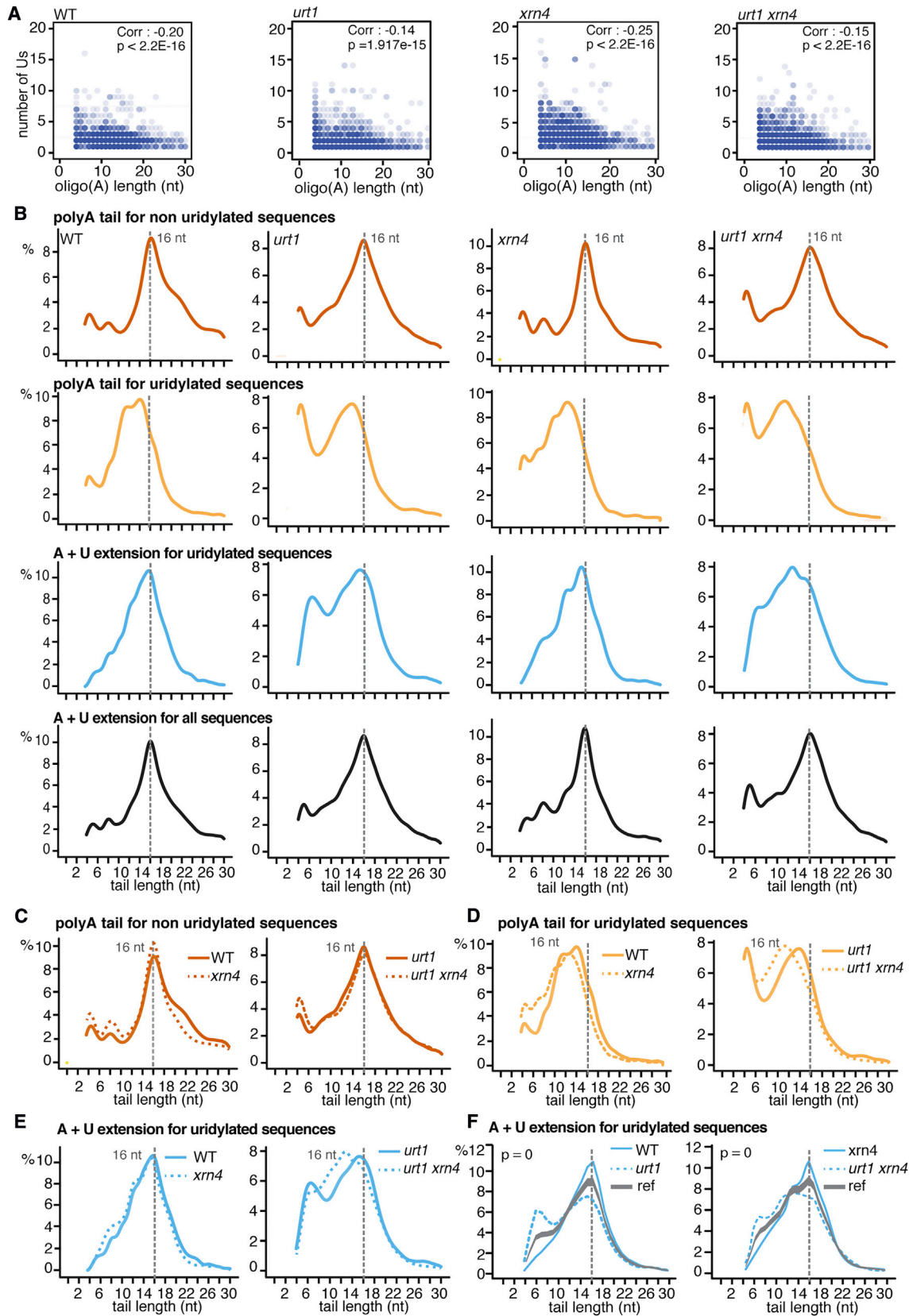
To further investigate the link between uridylation and deadenylation, the TAIL-seq datasets were analyzed by plotting the num-

ber of Us added to mRNA 3' ends against the size of the oligo(A) tails (Figure 4A). Despite relatively low Pearson correlation coefficients, p values inferior to $2E-15$ indicate that the inverse correlation observed between the size of the oligo(A) tails and the numbers of U added is significantly different from 0. In other words, the shorter the oligo(A) size, the more Us are added. This observation prompted us to compare the size distribution of oligo(A) tails between non-uridylated and uridylated mRNAs (Figure 4B). For non-uridylated mRNAs, the tail distribution of oligo(A) tails (i.e., As only, from four to 30 As) peaks at 16 nt (Figure 4B). The presence of short oligo(A)-tailed mRNAs in *Arabidopsis* was validated with a method devoid of any potential PCR bias (Figures S3A and S3B). As expected, oligo(A) tail size distribution is influenced by the lack of URT1 since a higher proportion of short oligo(A) tailed mRNAs accumulates in *urt1* and *urt1 xrn4* (Figures 4B–4E). This accumulation is likely underestimated because oligo(A) tails less than four As are excluded during TAIL-seq data processing (see Experimental Procedures). This observation confirms at genomic scale that excessively deadenylated mRNAs accumulate in absence of URT1, as we previously showed for model mRNAs (Sement et al., 2013).

Interestingly, plotting the distribution size of oligo(A) tails (As only) for uridylated sequences revealed a clear shift of the main peak by a few nucleotides toward smaller sizes as compared to non-uridylated sequences (Figures 4B and 4D). This shift is observed for all four genotypes: WT, *urt1*, *xrn4*, and *urt1 xrn4*. Importantly, the overall size distribution centered on 16 nt is restored in both WT and *xrn4* when the whole extensions (As + Us) for uridylated sequences are considered (Figures 4B and 4E). This restoration indicates that uridylation repairs deadenylated ends.

URT1 is expected to play a prominent role in this repair process since it is the main activity uridylating mRNAs in WT and *xrn4*. Indeed, a WT-like distribution for uridylated mRNAs is not observed neither in *urt1* nor *urt1 xrn4*, with a significant higher proportion of shorter tails as compared with WT and *xrn4* (Figures 4B, 4E, and 4F). This shows that, despite the inverse correlation between the size of the oligo(A) tails and the numbers of U observed in the absence of URT1 (Figure 4A), uridylation by URT1 remains essential to fully restore the size distribution observed for non-uridylated sequences. URT1-independent uridylyltransferase activity(ies) could be either inefficient in repairing deadenylated mRNA ends or unable to cope with the increase of excessively deadenylated mRNAs due to the absence of URT1. Either way, a functional URT1 is required to observe a similar size distribution of extension size for non-uridylated and uridylated oligo(A) mRNAs. Similar results were obtained by compiling 1,516, 1,152, 1,022, and 385 sequences for WT, *urt1*, *xrn4*, and *urt1 xrn4*, respectively, and for seven model mRNAs analyzed by 3' RACE PCR (Figure S3C), which validates the TAIL-seq data. Taken together, these results indicate that uridylation repairs deadenylated ends to restore the size distribution observed for non-uridylated sequences.

In addition, a significant increase in the density of reads representing short oligo(A) tails of uridylated mRNAs is detected by TAIL-seq and 3' RACE-PCR analyses in *xrn4* as compared with WT (Figures 4D and S3C). If uridylation restores the normal size distribution of deadenylated tails, we would expect that



(legend on next page)

the shorter oligo(A) tails observed in *xrn4* have longer U-extensions as compared to the U-extensions detected in WT. Indeed, in WT, 25% of U-extensions are longer than two Us, and only 7% of U-tails are longer than three Us. In *xrn4*, 42% of U-extensions are longer than 2 Us, while 19% are longer than 3 Us. Both the average U-tail size and the distribution of U-extensions are significantly different between WT and *xrn4* with $<2E-16$ and $5.5E-9$ p values for Mann-Whitney and chi-square tests, respectively. A similar, yet exacerbated, phenomenon was observed for the seven mRNAs analyzed by 3' RACE-PCR. Only 6% of U-tails are larger than three Us in WT, whereas 34% of U-tails are more than three Us in *xrn4* (p values for Mann-Whitney and chi-square tests, $7.4E-15$ and $2.851E-14$, respectively). Therefore, both TAIL-seq and 3' RACE-PCR data show that U-tails are significantly longer in *xrn4* as compared to WT, in line with a preliminary observation obtained with independent samples and for a limited number of mRNAs (Sement et al., 2013).

In conclusion, the most striking information gained through TAIL-seq analysis is that uridylation restores the oligo(A) size distribution observed for non-uridyated oligoadenylated mRNAs. U-extensions are larger in *xrn4*, compensating for the shorter oligo(A) tails observed when 5'-3' degradation is compromised.

PABP Binds to Uridylated mRNAs and Determines the Size of U-Extensions

The predominance of oligo(A) tails (<31 As) peaking around 16 nt for oligoadenylated mRNAs likely reveals the footprint of a factor bound to oligo(A) tails. A candidate for this binding activity is the cytoplasmic PolyA Binding Protein (PABP). PABP requires at least 12 nt for binding and can bind other homopolymers than poly(A) (Baejen et al., 2014; Eliseeva et al., 2013; Kini et al., 2015; Tuck and Tollervey, 2013). The *Arabidopsis* genome contains eight *PAB* genes, *PAB2*, *PAB4*, and *PAB8* showing high and broad expression in vegetative tissues (Belostotsky, 2003). PABPs are multifunctional proteins with major roles in mRNA stabilization and translation. Therefore, we did not use a reverse genetic strategy to validate a potential involvement of PABPs in the metabolism of uridyated oligo(A) tails. Rather, we used two complementary biochemical approaches. First, we tested whether PABP binds uridyated oligo(A) tails in vivo. To this end, we performed RNA immunoprecipitation (RIP) experiments using anti-PABP antibodies. The uridylation status of At1g24160 mRNAs in RNA samples extracted from immunoprecipitated fractions was determined by 3' RACE PCR in two biological replicates. Mock reactions, i.e., without anti-PABP antibodies, were used as negative controls (Figure 5A). 3' RACE-PCR products were obtained only from RNA samples extracted from immuno-

precipitated fractions (Figure 5B). Sequence analysis revealed that 27% of 51 clones correspond to uridyated At1g24160 mRNAs showing that PABP binds uridyated oligo(A) tails in vivo (Figure 5C). Interestingly, the sizes of A + U extensions for the immunoprecipitated mRNAs vary from 15 to 18 nt, with a median size of 17 nt. This size range fits well to the prevalent sizes observed for oligoadenylated mRNAs by TAIL-seq and 3' RACE-PCR. Next, we determine the impact of one of the constitutively expressed PABP (PAB2) on U-tail synthesis by URT1 in vitro using recombinant proteins (Figure 5D). To prevent the foldback of U-tails on a oligo(A) sequence that could interfere with the assay, we first used a non-adenylated 21-nt RNA substrate. As previously shown (Sement et al., 2013), URT1 adds large U-tails (>100 Us) to this RNA substrate when incubated in excess of UTP (1 mM). These U-tails of undefined sizes appear as large smears on acrylamide gels. Strikingly, adding PAB2 does not prevent the initial extension by URT1 but limits the number of added uridines to generate a product of defined length (40 nt) rather than the smear typically observed in absence of PAB2 (Figure 5E). Therefore, PAB2 can efficiently limit the extent of U-addition by URT1 in vitro. We then used a more physiological RNA substrate corresponding to the last 336 nt of *AGO1* mRNA plus 15 As. URT1 is able to uridylate this template as judged by the size increase observed by PAGE following incubation of the substrate with URT1 and UTP (Figure 5F). PAB2 efficiently blocks extension by uridine addition, likely by binding to the oligo(A) tail and preventing URT1 access. Taken together, these in vitro assays show that PAB2 is intrinsically able to limit uridine extension by URT1 and that an initial oligo(A) tail of 15 nt is sufficient for this inhibitory effect. Altogether, these results show that PABP can determine the size of U extensions added by URT1 and that PABP binds uridyated oligo(A) tails in vivo.

DISCUSSION

Our data reveal that uridylation repairs deadenylated mRNAs to restore a defined tail length, which allows for PABP binding. The detection of PABP bound to uridyated mRNAs may profoundly extend our view on the roles played by uridylation in mRNA metabolism. Previous studies have demonstrated that uridylation is linked to cytosolic mRNA degradation in eukaryotes (Lim et al., 2014; Morozov et al., 2010, 2012; Mullen and Marzluff, 2008; Rissland and Norbury, 2009; Slevin et al., 2014; Su et al., 2013). Such a destabilizing role for uridylation certainly exists as well in *Arabidopsis*. In fact, our current data do definitely not exclude the possibility that uridylation by URT1 could also induce mRNA degradation, besides its role in controlling the

Figure 4. Uridylation Repairs Deadenylated mRNAs

(A) Number of Us plotted against poly(A) tail length for uridyated sequences determined by TAIL-seq analysis. Pearson correlation coefficients were estimated between the poly(A) tail length and the number of Us.

(B) Distribution of tail sizes determined by TAIL-seq analysis. Plots display a smooth density estimate of the extension sizes (1D Gaussian kernel).

(C) Overlay of oligo(A) tail size distribution for non-uridyated mRNAs in WT and *xrn4*, and *urt1* and *urt1 xrn4*.

(D) Overlay of oligo(A) tail size distribution for uridyated mRNAs in WT and *xrn4*, and *urt1* and *urt1 xrn4*.

(E) Overlay of size distribution for A+U extension for uridyated mRNAs in WT and *xrn4*, and *urt1* and *urt1 xrn4*.

(F) Comparison of univariate density estimates with the *sm* R package for A+U extension for uridyated mRNAs between WT and *urt1*, and *xrn4* and *urt1 xrn4*. Grey bands display upper and lower end points of the reference (ref) band for equality.

Note that mRNAs with zero to three As are not considered during TAIL-seq data processing (see Supplemental Experimental Procedures).

See also Figure S3.

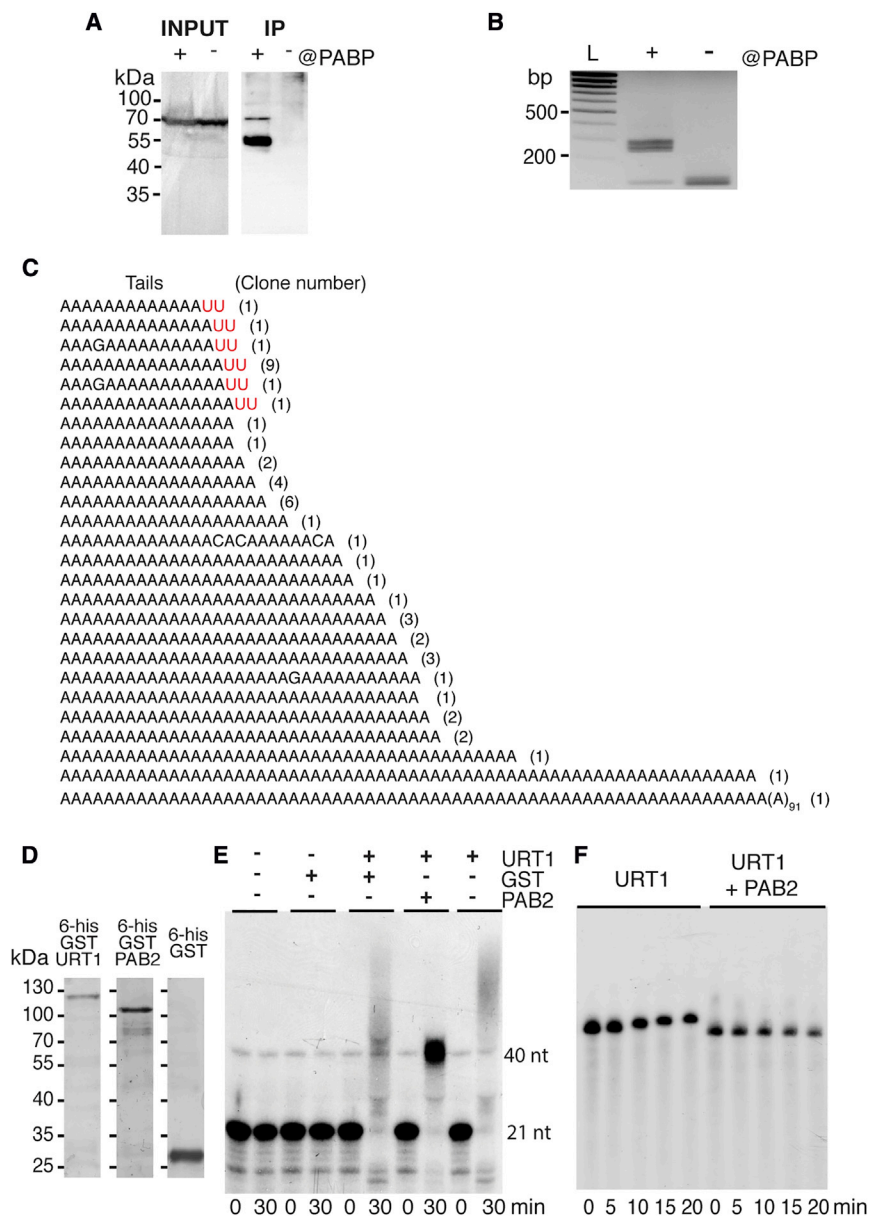


Figure 5. PABP Binds to Uridylated mRNAs In Vivo and Determines the Size of U-Extensions In Vitro

(A) Western blot analysis of PABP immunoprecipitation (IP) performed from WT plants.

(B) 3' RACE-PCR profiles for At1g24160 mRNAs co-precipitated with PABP.

(C) Tails of 51 3' RACE clones. Numbers of clone are indicated in brackets for each tail.

(D) Coomassie-blue-stained gels of 6-his-GST-URT1, 6-his-GST-PAB2, and GST expressed in *E. coli* and purified using Ni-NTA and glutathione Sepharose resins.

(E) Impact of PAB2 on U-tail synthesis by URT1 in vitro. GST-URT1 were incubated for 30 min with a non-adenylated 21-nt RNA 5'-labeled substrate and UTP (1 mM), and with or without GST-PAB2 or GST as indicated.

(F) PAB2 efficiently blocks uridine addition to a mRNA with a tail of 15 As. Time course of GST-URT1 incubation with UTP (1 mM), a 5' [³²P]-labeled 336-nt fragment of AGO1 mRNA tailed with 15 As, and with or without GST-PAB2.

extent of deadenylation. A plausible scenario based on our overall data would be that deadenylation would reach a stage determined by an oligo(A) size >13–15 As where uridylation competes with deadenylation (the “repair” step described here and involving PABP). Even if slowed down, deadenylation could still proceed and beyond a certain size, the repair is no longer effective to allow for PABP binding. These shorter uridyated tails could be recognized by decay factors to promote either by 5'-3' or 3'-5' degradation. However, this potential destabilizing role of URT1-mediated uridylation remains to be formally demonstrated. So far, we have observed that URT1-mediated uridylation on selected model mRNAs does not affect decay rates while preventing trimming of oligoadenylated mRNAs (Sement et al., 2013). By contrast, the second type of uridylation de-

tected by the TAIL-seq analysis in *urt1 xrn4* mutants does not protect deadenylated 3' ends and could be involved in mRNA destabilization. HESO1, a second uridylyltransferase identified in *Arabidopsis*, represents a good candidate for this alternative uridylation activity. Uridylation by HESO1 favors miRNAs and RISC-cleaved transcripts degradation (Ren et al., 2012, 2014; Zhao et al., 2012), and future experiments will reveal whether HESO1 also facilitates the degradation of mRNAs. However, URT1-mediated uridylation definitely plays an additional role in mRNA metabolism, and this is the primary focus of the present study.

The most straightforward interpretation of the data presented here is that a dynamic equilibrium between URT1 and the deadenylase activity(ies) could define the actual length of oligoadenylated mRNAs in *Arabidopsis*. This implies a two-step scenario. In a first step, URT1 needs to gain access to the 3' extremity of deadenylated mRNAs, possibly when the deadenylase switches between a processive to a distributive activity when the oligo(A) tails get shorter (Viswanathan et al., 2003). Alternatively, URT1 may intrinsically prefer short oligo(A) tails as recently shown for the human TUT4 and TUT7 (Lim et al., 2014). In a second step, uridylation would impede deadenylation according to one of the following possibilities: (1) the presence of one or two Us could directly hinder the recognition by deadenylases, (2) both the deadenylase and URT1 could compete for the oligoadenylated mRNA 3' extremity and URT1 would impede deadenylation by steric hindrance, (3) uridylation would favor the binding of a protective factor. These three possibilities are not mutually exclusive.

However, our present data support the latter mechanism since we observed that uridylation restores a size distribution of oligo(A) tails centered at 16 As.

Several lines of evidence indicate that a factor that binds uridylated mRNAs *in vivo* is PABP. First, PABPs have the capacity to bind other sequences than poly A tails (Baejen et al., 2014; Eliseeva et al., 2013; Kini et al., 2015; Tuck and Tollervey, 2013) and by combining PABP immunoprecipitation with 3' RACE, we demonstrate that PABP can bind uridylated oligo(A) tails in *Arabidopsis*. Second, after an initial step of uridylation, *Arabidopsis* PAB2 very efficiently limits U-extension of a non-adenylated RNA substrate by URT1 *in vitro*. This experiment shows that PAB2 does not inhibit URT1 activity directly but rather suggests that URT1 starts synthesizing a U-tail, which is bound by PAB2 once the tail reaches a defined length, which then prevents further uridylation by URT1. Importantly, URT1 is a distributive enzyme for the first added nucleotides (Sement et al., 2013). Hence, URT1 releases its RNA substrate after each U-addition, which likely facilitates binding of PABP. Under the conditions used, 19 Us are added. Taking into consideration that two As are present at the 3' end of the RNA substrate, a total of 21 U + As is present before URT1 ceases to elongate the tail. Considering that *in vitro*, tail length might be biased by several parameters such as the nucleotide composition of the tail, the absence of a competing deadenylase activity and the high concentration of URT1 and substrates (RNA and nucleotides), a tail length of 21 nt is in good adequation with the oligo(A) length determined *in vivo*. Finally, PAB2 prevents URT1-mediated uridylation of a reporter sequence with an already existing tail of 15 As. Interestingly, human PABPC1 also suppresses uridylation of tails of 25 or 50 As by TUT4 and TUT7 *in vitro* (Lim et al., 2014). Taken together, these data support the idea that PABP interacts with uridylated oligo(A) tails and that PABP will inhibit URT1 elongation once a sufficient length is attained for its binding. This also explains the observed inverse correlation between the size of the oligo(A) tails and the numbers of Us added, and the restoration of oligo(A) size distribution by uridylation. Interestingly, the median size of uridylated oligo(A) tails (A + U) immunoprecipitated with PAB2 is 17 nt, which fits remarkably well to the peak of oligo(A) tails detected by TAIL-seq analysis. A size of 17 As may seem modest given that PABP can occupy up to 27 As (reviewed in Eliseeva et al., 2013). However, the minimal oligo(A) size bound by PABP is 12 As (Sachs et al., 1987). Hence, the peak centered at 16 nt observed by TAIL-seq may reflect the equilibrium set by competing PABP, URT1, and deadenylases.

The recognition of uridylated oligo(A) tails by PABP raises interesting questions on the biological roles of uridylation. URT1-mediated uridylation could be both part of the general mRNA degradation pathway and play also other roles in mRNA metabolism. These additional roles may vary with the different subcellular localization of uridylated mRNAs and, therefore, with the distinct and particular protein environment. URT1 is not only diffusely distributed in the cytosol, but also is localized in both P-bodies and stress granules (Sement et al., 2013). In stress granules, URT1 and PABP could play an obvious role in mRNA storage through URT1-mediated protection of deadenylated mRNA 3' ends by PABP binding. Whether and how URT1 influences mRNA fate in P-bodies is unknown at present.

P-bodies components include the decapping machinery, the 5'-3' exoribonuclease and deadenylases but no detectable PABP. Uridylation by URT1 could yet favor 5' to 3' polarity of degradation in P-bodies either by directly impeding deadenylase activities and/or promoting decapping. Another protein than PABP could also recognize uridylated oligo(A) tails in P-bodies. A 5' to 3' polarization of degradation could be important to prevent the formation of aberrant transcripts such as mRNAs excessively trimmed by deadenylases. These aberrant RNAs could be substrates of the potent siRNA pathway of plants (Zhang et al., 2015). However, the most intriguing question raised by the binding of PABP to uridylated mRNAs is a potential role of URT1-mediated uridylation on polysomes. We have previously shown that uridylated transcripts are indeed present on polysomes, and that excessive deadenylation occurs on polysomal mRNAs in *urt1* (Sement et al., 2013). The protection conferred by URT1 to 3' ends of polysomal mRNAs could be important for the 5'-3' polarity of degradation while mRNAs are still engaged on polysomes. Indeed, co-translational degradation of mRNAs emerges as a conserved feature in eukaryotes (Hu et al., 2009; Merret et al., 2015; Pelechano et al., 2015). Alternatively, binding of PABP to uridylated oligo(A) tails could affect their translatability. At present, it cannot be excluded that deadenylated uridylated mRNAs bound by PABP are actively translated. However, initial experiments in *Xenopus* oocytes and *A. nidulans* suggests that uridylation is linked with translation inhibition (Lapointe and Wickens, 2013; Morozov et al., 2012). Whether this inhibitory role is conserved in *Arabidopsis* and/or whether URT1-mediated uridylation restores translation of deadenylated mRNA constitutes an exciting area for future investigation. In fact, we are just beginning to appreciate the functions conferred by uridylation in mRNA metabolism and their diversity across eukaryotes. The finding that uridylation repairs deadenylated ends to restore a binding site for PABP constitutes a key step toward our general understanding of the overall function of uridylation in mRNA metabolism.

EXPERIMENTAL PROCEDURES

Material

Arabidopsis thaliana plants were of Col-0 ecotype and grown on soil with 16-hr-light/8-hr-darkness cycles. *urt1-1* (Salk_087647C) and *xrn4-3* (SALK_014209) have been previously described (Gazzani et al., 2004; Sement et al., 2013) and were crossed to produce *urt1 xrn4*. myc-URT1-expressing lines were produced by transforming the *urt1-1* mutant by the floral dip method with the genomic sequence of URT1 cloned in pGWB621. All primer sequences and vectors are detailed in Supplemental Experimental Procedures.

Western Blotting

Immunoblots were incubated with anti-URT1 antibodies raised in rabbits against the full-length recombinant URT1, or with anti-myc (Roche), anti-NTRB (kind gift from Géraldine Bonnard), or anti-PAB2 (kind gift from Cécile Bousquet-Antonelli) antibodies in Tris-buffered saline (TBS); 5% (w/v) milk; 0.02% (v/v) Tween 20. Following incubation with horseradish-peroxidase-coupled secondary antibodies and Lumi-Light Western Blotting Substrate (Roche), signals were recorded using the Fusion-FX system (Fisher Biotech).

3' RACE-PCR

The 3' RACE PCR protocol used to sequence mRNAs 3' ends is detailed in Sement and Gagliardi (2014). See Supplemental Experimental Procedures for an outline of the protocol.

TAIL-Seq

TAIL-seq libraries were prepared from WT, *urt1*, *xrn4*, and *urt1 xrn4* 2-week-old seedlings according to Chang et al. (2014). After rRNA depletion, RNAs were ligated to a biotinylated 3' adaptor and partially digested by RNase T1. RNA 3' fragments were purified with streptavidin beads, phosphorylated, and gel purified (500–1,500 nt). The purified RNAs were ligated to a 5' adaptor, reverse transcribed, and amplified by PCR. PCR products were purified and sequenced on the Illumina HiSeq 2500 (50 × 240 bp paired end run). Sequences were processed using the Base calls acquired from HiSeq 2500 after processing by Illumina CASAVA-1.8.2. A detailed protocol of both library preparation and data processing are provided in Supplemental Experimental Procedures.

Small RNA Library Preparation and Sequencing

Small RNA libraries were generated from 3 μg of total RNA extracted with TRIzol reagent (Invitrogen) from WT and *urt1* 2-week-old seedlings, two biological replicates each. Small RNA libraries were produced using the Illumina Small RNA TruSeq protocol and sequenced using a HiSeq 2000 sequencer. Sequences were processed using the base calls acquired from HiSeq 2000 after processing by Illumina CASAVA-1.8.2. A full protocol of the data processing is provided in Supplemental Experimental Procedures.

Expression and Purification of Recombinant Proteins

6his-GST-URT1, 6his-GST-PAB2, and GST were produced in BL21(DE3) cells grown at 17°C. Cells were disrupted by sonication in 20 mM MOPS (pH 7.5), 250 mM KCl, 15% (v/v) glycerol, 1 mM DTT, and 0.1% (v/v) Tween 20 in presence of protease inhibitors (Roche). Recombinant proteins were purified on Ni-NTA resin followed by glutathione affinity chromatography. Purified proteins were dialyzed against 20 mM MOPS (pH 7.5), 100 mM NaCl, 15% (v/v) glycerol, 0.1% (v/v) Tween 20. Aliquots were snap-frozen in liquid nitrogen and stored at –80°C.

Activity Assays

In vitro assays shown in Figure 5 contained 100 nM of GST-URT1, 20 mM MOPS (pH 7.5), 100 mM NaCl, 15% (v/v) glycerol, 0.1% (v/v) Tween 20, 1 mM MgCl₂, 0.5 μg/μl BSA, and 1 mM UTP. For Figure 5E, GST-URT1 was incubated for 30 min with or without GST-PAB2 (20 nM) or GST (20 nM) and with a non-adenylated 21-nt RNA substrate labeled by T4 Polynucleotide Kinase (NEB) and [³²P]-ATP. Reaction products were separated by denaturing 5% (w/v) polyacrylamide gel electrophoresis before autoradiography. For Figure 5F, GST-URT1 was incubated for different time points with or without GST-PAB2 (20 nM) and with the last 336 nt of AGO1 mRNA plus 15 As labeled by T4 Polynucleotide Kinase (NEB) and [³²P]-ATP. Reaction products were separated by denaturing 17% (w/v) polyacrylamide gel electrophoresis before autoradiography.

RNA Immunoprecipitation

For PABP immunoprecipitation, 300 mg of flowers were ground in 1 ml of 50 mM Tris-HCl (pH 8.0), 150 mM NaCl, 1% Triton X-100, 1 × Complete Protease Inhibitor EDTA free (Roche), and 10 mM ribonucleoside-vanadyl complex (NEB). Lysates were clarified by centrifugation at 4°C at 16,000 × g for 5 min, incubated with anti-PABP antibodies, and purified using magnetic protein A MicroBeads (Miltenyi Biotech) according to the manufacturer's instruction. Protein-RNA complexes were directly eluted from magnetic beads using 100 μl of 20 mM MOPS (pH 7.5), 10 mM NaCl, and 0.1% Triton X-100. 20 μl of the eluates was separated by SDS-PAGE electrophoresis and analyzed by western blotting. 5 μg of yeast total RNA was added to the remaining 80 μl eluates, and RNA was purified using RNeasy MinElute columns (QIAGEN). 3' end extremities were analyzed by the modified 3' RACE-PCR protocol previously described.

ACCESSION NUMBERS

Sequenced reads have been deposited in the NCBI Gene Expression Omnibus (GEO): GSE72458.

SUPPLEMENTAL INFORMATION

Supplemental Information includes Supplemental Experimental Procedures and three figures and can be found with this article online at <http://dx.doi.org/10.1016/j.celrep.2016.02.060>.

AUTHOR CONTRIBUTIONS

H.Z. designed, conducted, and analyzed experiments and performed all bioinformatics analyses. H.S., E.F., F.M.S., P.M., and B.S. performed and analyzed experiments. D.G. designed and analyzed experiments and supervised the project. The manuscript was written by D.G. and H.Z.

ACKNOWLEDGMENTS

We thank V. Narry Kim, Jaechul Lim, and Hyeshik Chang (Seoul, Korea) for advice on TAIL-seq library construction. We also thank Cécile Bousquet-Antonielli and Jean-Marc Deragon (Perpignan, France) for providing the anti-PAB2 antibodies. This work was supported by the Center National de la Recherche Scientifique (CNRS) and a research grant from the French National Research Agency as part of the "Investments for the future" program in the framework of the LABEX ANR-10-LABX-0036_NETRINA to D.G.

Received: August 26, 2015

Revised: December 8, 2015

Accepted: February 11, 2016

Published: March 10, 2016

REFERENCES

- Baejen, C., Torkler, P., Gressel, S., Essig, K., Söding, J., and Cramer, P. (2014). Transcriptome maps of mRNP biogenesis factors define pre-mRNA recognition. *Mol. Cell* 55, 745–757.
- Belostotsky, D.A. (2003). Unexpected complexity of poly(A)-binding protein gene families in flowering plants: three conserved lineages that are at least 200 million years old and possible auto- and cross-regulation. *Genetics* 163, 311–319.
- Chang, H., Lim, J., Ha, M., and Kim, V.N. (2014). TAIL-seq: genome-wide determination of poly(A) tail length and 3' end modifications. *Mol. Cell* 53, 1044–1052.
- Charlesworth, A., Meijer, H.A., and de Moor, C.H. (2013). Specificity factors in cytoplasmic polyadenylation. *Wiley Interdiscip. Rev. RNA* 4, 437–461.
- Eliseeva, I.A., Lyabin, D.N., and Ovchinnikov, L.P. (2013). Poly(A)-binding proteins: structure, domain organization, and activity regulation. *Biochemistry (Mosc.)* 78, 1377–1391.
- Gazzani, S., Lawrenson, T., Woodward, C., Headon, D., and Sablowski, R. (2004). A link between mRNA turnover and RNA interference in Arabidopsis. *Science* 306, 1046–1048.
- Hu, W., Sweet, T.J., Chamnongpol, S., Baker, K.E., and Collier, J. (2009). Co-translational mRNA decay in *Saccharomyces cerevisiae*. *Nature* 461, 225–229.
- Kini, H.K., Silverman, I.M., Ji, X., Gregory, B.D., and Liebhaber, S.A. (2015). Cytoplasmic poly(A) binding protein-1 binds to genomically encoded sequences within mammalian mRNAs. *RNA* 22, 61–74.
- Knüsel, S., and Roditi, I. (2013). Insights into the regulation of GPEET procyclin during differentiation from early to late procyclic forms of *Trypanosoma brucei*. *Mol. Biochem. Parasitol.* 191, 66–74.
- Lange, H., Sement, F.M., Canaday, J., and Gagliardi, D. (2009). Polyadenylation-assisted RNA degradation processes in plants. *Trends Plant Sci.* 14, 497–504.
- Lapointe, C.P., and Wickens, M. (2013). The nucleic acid-binding domain and translational repression activity of a *Xenopus* terminal uridylyl transferase. *J. Biol. Chem.* 288, 20723–20733.

- Lee, M., Kim, B., and Kim, V.N. (2014). Emerging roles of RNA modification: m(6)A and U-tail. *Cell* **158**, 980–987.
- Lim, J., Ha, M., Chang, H., Kwon, S.C., Simanshu, D.K., Patel, D.J., and Kim, V.N. (2014). Uridylation by TUT4 and TUT7 marks mRNA for degradation. *Cell* **159**, 1365–1376.
- Malecki, M., Viegas, S.C., Carneiro, T., Golik, P., Dressaire, C., Ferreira, M.G., and Arraiano, C.M. (2013). The exoribonuclease Dis3L2 defines a novel eukaryotic RNA degradation pathway. *EMBO J.* **32**, 1842–1854.
- Mangus, D.A., Evans, M.C., and Jacobson, A. (2003). Poly(A)-binding proteins: multifunctional scaffolds for the post-transcriptional control of gene expression. *Genome Biol.* **4**, 223.
- Merret, R., Nagarajan, V.K., Carpentier, M.-C., Park, S., Favory, J.-J., Descombin, J., Picart, C., Charnig, Y.-Y., Green, P.J., Deragon, J.-M., and Bousquet-Antonelli, C. (2015). Heat-induced ribosome pausing triggers mRNA co-translational decay in *Arabidopsis thaliana*. *Nucleic Acids Res.* **43**, 4121–4132.
- Morozov, I.Y., Jones, M.G., Razak, A.A., Rigden, D.J., and Caddick, M.X. (2010). CUCU modification of mRNA promotes decapping and transcript degradation in *Aspergillus nidulans*. *Mol. Cell Biol.* **30**, 460–469.
- Morozov, I.Y., Jones, M.G., Gould, P.D., Crome, V., Wilson, J.B., Hall, A.J.W., Rigden, D.J., and Caddick, M.X. (2012). mRNA 3' tagging is induced by nonsense-mediated decay and promotes ribosome dissociation. *Mol. Cell Biol.* **32**, 2585–2595.
- Mullen, T.E., and Marzluff, W.F. (2008). Degradation of histone mRNA requires oligouridylation followed by decapping and simultaneous degradation of the mRNA both 5' to 3' and 3' to 5'. *Genes Dev.* **22**, 50–65.
- Munoz-Tello, P., Rajappa, L., Coquille, S., and Thore, S. (2015). Polyuridylation in Eukaryotes: A 3'-End Modification Regulating RNA Life. *BioMed Res. Int.* **2015**, 968127.
- Norbury, C.J. (2013). Cytoplasmic RNA: a case of the tail wagging the dog. *Nat. Rev. Mol. Cell Biol.* **14**, 643–653.
- Pelechano, V., Wei, W., and Steinmetz, L.M. (2015). Widespread Co-translational RNA Decay Reveals Ribosome Dynamics. *Cell* **161**, 1400–1412.
- Ren, G., Chen, X., and Yu, B. (2012). Uridylation of miRNAs by hen1 suppressor1 in *Arabidopsis*. *Curr. Biol.* **22**, 695–700.
- Ren, G., Xie, M., Zhang, S., Vinovskis, C., Chen, X., and Yu, B. (2014). Methylation protects microRNAs from an AGO1-associated activity that uridylates 5' RNA fragments generated by AGO1 cleavage. *Proc. Natl. Acad. Sci. USA* **111**, 6365–6370.
- Rissland, O.S., and Norbury, C.J. (2009). Decapping is preceded by 3' uridylation in a novel pathway of bulk mRNA turnover. *Nat. Struct. Mol. Biol.* **16**, 616–623.
- Sachs, A.B., Davis, R.W., and Kornberg, R.D. (1987). A single domain of yeast poly(A)-binding protein is necessary and sufficient for RNA binding and cell viability. *Mol. Cell Biol.* **7**, 3268–3276.
- Sement, F.M., and Gagliardi, D. (2014). Detection of uridylated mRNAs. *Methods Mol. Biol.* **1125**, 43–51.
- Sement, F.M., Ferrier, E., Zuber, H., Merret, R., Alioua, M., Deragon, J.-M., Bousquet-Antonelli, C., Lange, H., and Gagliardi, D. (2013). Uridylation prevents 3' trimming of oligoadenylated mRNAs. *Nucleic Acids Res.* **41**, 7115–7127.
- Slevin, M.K., Meaux, S., Welch, J.D., Bigler, R., Miliani de Marval, P.L., Su, W., Rhoads, R.E., Prins, J.F., and Marzluff, W.F. (2014). Deep sequencing shows multiple oligouridylations are required for 3' to 5' degradation of histone mRNAs on polyribosomes. *Mol. Cell* **53**, 1020–1030.
- Su, W., Slepnev, S.V., Slevin, M.K., Lyons, S.M., Ziemniak, M., Kowalska, J., Darzynkiewicz, E., Jemielity, J., Marzluff, W.F., and Rhoads, R.E. (2013). mRNAs containing the histone 3' stem-loop are degraded primarily by decapping mediated by oligouridylation of the 3' end. *RNA* **19**, 1–16.
- Thomas, M.P., Liu, X., Whangbo, J., McCrossan, G., Sanborn, K.B., Basar, E., Walch, M., and Lieberman, J. (2015). Apoptosis triggers specific, rapid, and global mRNA decay with 3' uridylated intermediates degraded by DIS3L2. *Cell Rep.* **11**, 1079–1089.
- Tu, B., Liu, L., Xu, C., Zhai, J., Li, S., Lopez, M.A., Zhao, Y., Yu, Y., Ramachandran, V., Ren, G., et al. (2015). Distinct and cooperative activities of HESO1 and URT1 nucleotidyl transferases in microRNA turnover in *Arabidopsis*. *PLoS Genet.* **11**, e1005119.
- Tuck, A.C., and Tollervey, D. (2013). A transcriptome-wide atlas of RNP composition reveals diverse classes of mRNAs and lncRNAs. *Cell* **154**, 996–1009.
- Viegas, S.C., Silva, I.J., Apura, P., Matos, R.G., and Arraiano, C.M. (2015). Surprises in the 3'-end: 'U' can decide too!. *FEBS J.* **282**, 3489–3499.
- Viswanathan, P., Chen, J., Chiang, Y.-C., and Denis, C.L. (2003). Identification of multiple RNA features that influence CCR4 deadenylation activity. *J. Biol. Chem.* **278**, 14949–14955.
- Wang, X., Zhang, S., Dou, Y., Zhang, C., Chen, X., Yu, B., and Ren, G. (2015). Synergistic and independent actions of multiple terminal nucleotidyl transferases in the 3' tailing of small RNAs in *Arabidopsis*. *PLoS Genet.* **11**, e1005091.
- Zhang, X., Zhu, Y., Liu, X., Hong, X., Xu, Y., Zhu, P., Shen, Y., Wu, H., Ji, Y., Wen, X., et al. (2015). Plant biology. Suppression of endogenous gene silencing by bidirectional cytoplasmic RNA decay in *Arabidopsis*. *Science* **348**, 120–123.
- Zhao, Y., Yu, Y., Zhai, J., Ramachandran, V., Dinh, T.T., Meyers, B.C., Mo, B., and Chen, X. (2012). The *Arabidopsis* nucleotidyl transferase HESO1 uridylates unmethylated small RNAs to trigger their degradation. *Curr. Biol.* **22**, 689–694.